G Protein-Coupled Receptor-Mediated Activation of p110{beta} by G{beta}{gamma} Is Required for Cellular Transformation and Invasiveness

Hashem A. Dbouk, Oscar Vadas, Aliaksei Shymanets, John E. Burke, Rachel S. Salamon, Bassem D. Khalil, Mathew O. Barrett, Gary L. Waldo, Chinmay Surve, Christine Hsueh, Olga Perisic, Christian Harteneck, Peter R. Shepherd, T. Kendall Harden, Alan V. Smrcka, Ronald Taussig, Anne R. Bresnick, Bernd Nürnberg, Roger L. Williams and Jonathan M. Backer (4 December 2012)

Science Signaling **5** (253), ra89. [DOI: 10.1126/scisignal.2003264]

CELL BIOLOGY

G Protein–Coupled Receptor–Mediated Activation of p110β by Gβγ Is Required for Cellular Transformation and Invasiveness

Hashem A. Dbouk,[1]* Oscar Vadas,[2]* Aliaksei Shymanets,[3] John E. Burke,[2] Rachel S. Salamon,[1] Bassem D. Khalil,[1] Mathew O. Barrett,[4] Gary L. Waldo,[4] Chinmay Surve,[5] Christine Hsueh,[6] Olga Perisic,[2] Christian Harteneck,[3] Peter R. Shepherd,[7] T. Kendall Harden,[4] Alan V. Smrcka,[5] Ronald Taussig,[8] Anne R. Bresnick,[6] Bernd Nürnberg,[3] Roger L. Williams,[2†] Jonathan M. Backer[1†]

Synergistic activation by heterotrimeric guanine nucleotide–binding protein (G protein)–coupled receptors (GPCRs) and receptor tyrosine kinases distinguishes p110β from other class IA phosphoinositide 3-kinases (PI3Ks). Activation of p110β is specifically implicated in various physiological and pathophysiological processes, such as the growth of tumors deficient in phosphatase and tensin homolog deleted from chromosome 10 (PTEN). To determine the specific contribution of GPCR signaling to p110β-dependent functions, we identified the site in p110β that binds to the Gβγ subunit of G proteins. Mutation of this site eliminated Gβγ-dependent activation of PI3Kβ (a dimer of p110β and the p85 regulatory subunit) in vitro and in cells, without affecting basal activity or phosphotyrosine peptide–mediated activation. Disrupting the p110β-Gβγ interaction by mutation or with a cell-permeable peptide inhibitor blocked the transforming capacity of PI3Kβ in fibroblasts and reduced the proliferation, chemotaxis, and invasiveness of PTEN-null tumor cells in culture. Our data suggest that specifically targeting GPCR signaling to PI3Kβ could provide a therapeutic approach for tumors that depend on p110β for growth and metastasis.

INTRODUCTION

Signaling by class I phosphoinositide 3-kinases (PI3Ks) is commonly enhanced in tumors by gene amplification, activating mutations, or the inactivation of phosphatase and tensin homolog deleted from chromosome 10 (PTEN), a tumor suppressor lipid phosphatase (*1*). Class I PI3Ks produce phosphatidylinositol-3,4,5-trisphosphate (PIP_3) in cells and stimulate proliferation, survival, and motility. The class IA enzymes are obligate heterodimers consisting of distinct catalytic (p110) subunits bound to the same regulatory (p85) subunits (*2*, *3*). Among the three class IA PI3Ks, the *PIK3CB* gene product p110β is unique because it can be activated both by receptor tyrosine kinases (RTKs) and downstream of heterotrimeric guanine nucleotide–binding protein (G protein)–coupled receptors (GPCRs) through direct binding to Gβγ subunits (*4*–*7*). The development of PTEN-deficient prostate cancer specifically depends on the activity of the p110β-p85 dimer (referred to as PI3Kβ), but the mechanism for this specificity is currently unknown (*8*–*11*). Whether GPCRs have a role in PI3Kβ-mediated transformation of PTEN-null cells has remained an open question because of the lack of tools to specifically probe the Gβγ-PI3Kβ interaction.

Defining the role of Gβγ in activating effectors such as p110β is challenging because of the transient nature of interactions between the two and because of the lack of a distinct Gβγ-binding motif that could be used to identify its target binding sites. This contrasts with the mechanism of activation of PI3Ks by RTKs, which involves high-affinity interactions that have been well characterized (*12*, *13*). To investigate the mechanism of p110β activation downstream of GPCRs by Gβγ, and to define the role of this interaction in p110β signaling in cells, we have identified the Gβγ-binding site on p110β. We took two parallel approaches, the first based on an analysis of sequence conservation and the second with hydrogen-deuterium exchange mass spectrometry (HDX-MS). Both approaches identified the same region, enabling us to generate a p110β mutant that remained sensitive to stimulation by RTKs but did not respond to activation by Gβγ. This mutant enabled us to interrogate the physiological importance of p110β activation downstream of GPCRs by Gβγ and to define a critical role for this interaction in the cellular transformation, proliferation, and invasiveness of PTEN-null tumor cells.

RESULTS

Identification of the Gβγ-binding site in p110β

We previously showed that the adaptor-binding, Ras-binding, and C2 domains of p110β are not responsible for its activation by Gβγ subunits (*14*). For this reason, we compared the remainder of the p110β sequence with those of p110α and p110δ, which are insensitive to stimulation by Gβγ, to look for sequence differences that might account for the selective activation of p110β by Gβγ. Whereas the helical and kinase domains of all three

[1]Department of Molecular Pharmacology, Albert Einstein College of Medicine, Bronx, NY 10461, USA. [2]MRC Laboratory of Molecular Biology, Cambridge CB2 0QH, UK. [3]Department of Pharmacology and Experimental Therapy, Institute for Pharmacology and Toxicology and Interfaculty Center of Pharmacogenomics and Pharma Research Eberhard-Karls-Universität Tübingen, Tübingen 72074, Germany. [4]Department of Pharmacology, University of North Carolina School of Medicine, Chapel Hill, NC 27599, USA. [5]Department of Pharmacology and Physiology, University of Rochester School of Medicine and Dentistry, Rochester, NY 14642, USA. [6]Department of Biochemistry, Albert Einstein College of Medicine, Bronx, NY 10461, USA. [7]Department of Molecular Medicine and Pathology, University of Auckland, Auckland 1142, New Zealand. [8]Department of Pharmacology, University of Texas Southwestern Medical Center, Dallas, TX 75390, USA.
*These authors contributed equally to this work.
†To whom correspondence should be addressed. E-mail: rlw@mrc-lmb.cam.ac.uk (R.L.W.); jonathan.backer@einstein.yu.edu (J.M.B.)

isoforms display high sequence similarity, we identified a 24–amino acid residue nonconserved region (residues 514 to 537) in the linker between the C2 domain and the helical domain of p110β (Fig. 1A and fig. S1). The central portion of this segment is not visible in the crystal structure of p110β, presumably because it is disordered, but it is part of a surface-accessible loop (*15*).

In parallel, we used an empirical approach, HDX-MS, to experimentally identify the p110β-Gβγ interaction sites. HDX-MS is a powerful technique to monitor protein dynamics, protein-protein interactions, and protein-lipid interactions (*16*–*19*). For HDX-MS measurements, we used two experimental setups, one with soluble Gβγ (Gγ-C68S) (Fig. 1, B and C) and another with lipid-modified Gβγ in the presence of membranes (fig. S2). To enhance the stability of interaction between the p110β-p85 dimer and soluble Gβγ in solution, we produced a heterotrimer containing p110β, Gγ-C68S, and a chimeric construct containing Gβ covalently linked to a fragment of p85α containing the C-terminal Src homology 2 (SH2) domain and the coiled-coil domain (iSH2-cSH2) (Fig. 1B). This heterotrimer formed a stable complex that could be stimulated by both a platelet-derived growth factor receptor (PDGFR)–derived bis-phosphopeptide (pY) and $G\beta_1\gamma_2$ subunits (Gβγ) (fig. S3A). When we compared differences in the HDX rates of p110β peptides between the heterotrimeric fusion complex and the wild-type p110β–p85α-icSH2 heterodimer, we identified two stretches that were more protected in the fusion complex (Fig. 1C and fig. S3, B and C). The first potential Gβγ-binding site, containing residues 518 to 538, matched very well with the region mapped by sequence analysis. The second protected region, amino acids 557 to 578, lies underneath the C2-helical linker. Changes in this region are likely a result of indirect effects from the binding of Gβγ to the linker above it. The same regions of p110β binding to Gβγ were identified with full-length PI3Kβ and lipidated Gβγ, with liposomes to stabilize the interactions (fig. S2, C and D, and tables S1 to S6). Taken together, the sequence analysis and HDX-MS data suggested that the region of p110β spanning residues 518 to 537 was the Gβγ-binding site.

To test whether this region was involved in Gβγ-mediated regulation of p110β, we designed a loop-swap p110β mutant in which these 24 amino acid residues were replaced with the corresponding region of p110δ (Fig. 1D). We also mutated residues

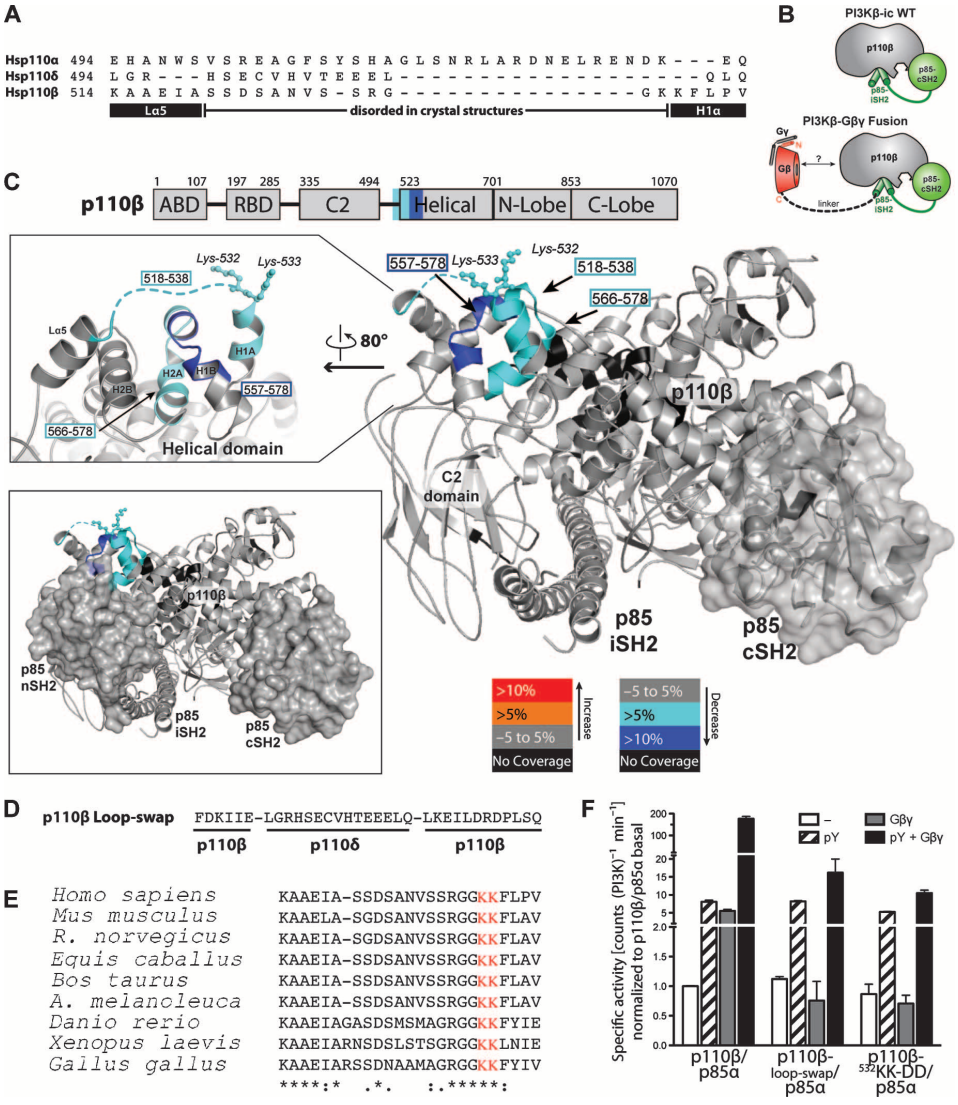

Fig. 1. Mapping of the Gβγ-binding site on p110β by sequence analysis and HDX-MS. (**A**) Sequence alignment of the C2 domain–helical domain linker region of p110α, β, and δ. The black rectangles denote helices in the p110β structure, and the black line represents the disordered region. (**B**) Cartoon illustration of the p110β–p85α-icSH2 wild-type (WT) heterodimer and the p110β–Gβ-p85α-icSH2–Gγ-C68S fusion heterotrimer (fusion) used for the HDX-MS experiments. (**C**) Domains of p110β are outlined and colored according to the legend for changes associated with the presence of Gβγ. Regions in p110β and p85α-icSH2 that showed >0.5 dalton and >5% changes in deuteration extent between the WT and fusion complexes were mapped on the p110β–p85β–icSH2 model (PDB: 2y3a, right panel). The loop region between the C2 domain and the helical domain is represented as a dotted line because it is not ordered in the structure. Residues corresponding to human p110β K532 and K533 are represented with balls and sticks. Top left, a close-up view of the p110β region in which changes in deuteration extent as a result of the presence of Gβγ were detected. Bottom left, a model for the p110β–p85α-nicSH2 generated by combining the structures of p110β–p85β-icSH2 (PDB: 2Y3A) and p85α–nSH2 (PDB: 3HHM). The nSH2 and cSH2 domains of p85 are shown as surface representations. The p85α-nSH2 position is based on the structure of p110α, although there is no unambiguous evidence that nSH2 adopts exactly the same position when in complex with p110β. (**D**) Sequence of the loop-swap mutant of p110β. (**E**) Alignment of p110β zoologs in the region of the C2-helical linker. (**F**) Activities of WT PI3Kβ and the loop-swap and ^{532}KK-DD mutants purified from insect cells, in the presence of pY peptide (pY) and lipidated Gβγ. Activities were expressed relative to the basal activity of PI3Kβ, which was normalized to 1. Graph shows the activity ± SD of three independent experiments.

lysines 532 and 533 (^{532}KK) in the p110β loop, which are highly conserved among p110β from different species but not between p110β and p110α or p110δ and which are ordered in the p110β crystal structure (Fig. 1E) (*15*). Replacement of the p110β loop with that of p110δ or mutation of ^{532}KK to DD had no effect on the in vitro basal kinase activity of PI3Kβ in assays with purified enzyme from insect cells (Fig. 1F) or in assays with enzyme immunopurified from mammalian cells (fig. S4, A and B). However, whereas wild-type PI3Kβ was markedly activated by the addition of Gβγ, neither the ^{532}KK-DD mutant nor the loop-swap mutant of PI3Kβ was activated by Gβγ (Fig. 1F and fig. S4, A and B). Wild-type and mutant enzymes were activated to a similar extent by pY (Fig. 1F and fig. S4, A and B), even though the mutation sits close to the predicted p85-nSH2–binding site (Fig. 1C) (*20*). Similar results were obtained with a ^{514}KAAEI-DAAKA mutant of p110β, which targets the N-terminal end of the loop (fig. S4C). The degree of activation of PI3Kβ by pY and Gβγ (Fig. 1) was consistent with previous studies with baculovirally expressed PI3Kβ purified from insect cells (*7*, *15*), although it was substantially greater than that seen with PI3Kβ immunopurified from transfected mammalian cells (fig. S4). These differences in fold activation may reflect the influences of assay conditions (see Supplementary Materials), N-terminal tags on basal activity, or the presence of an antibody bound to the immunopurified enzyme (*2*, *21*).

Role of Gβγ-mediated activation of p110β in signaling, transformation, and cell motility

To measure the effect of the p110β mutation on signaling to the serine and threonine kinase Akt, we transfected human embryonic kidney (HEK) 293E cells with plasmids encoding the wild-type or ^{532}KK-DD mutant p110β together with plasmids encoding p85α and myc-tagged Akt (myc-Akt), with or without plasmids encoding $G\beta_1\gamma_2$ subunits, which activate p110β in vitro (*22*). Gβγ-dependent Akt activation in this system was specifically inhibited by the p110β inhibitor TGX-221 and therefore reflected Gβγ-mediated stimulation of p110β (fig. S5A). Whereas cells containing wild-type PI3Kβ showed a marked increase in the abundance of Akt activated by phosphorylation at Thr^{308} (pT^{308}-Akt) in the presence of exogenous Gβγ subunits, cells transfected with plasmid encoding the ^{532}KK-DD mutant PI3Kβ showed a complete loss

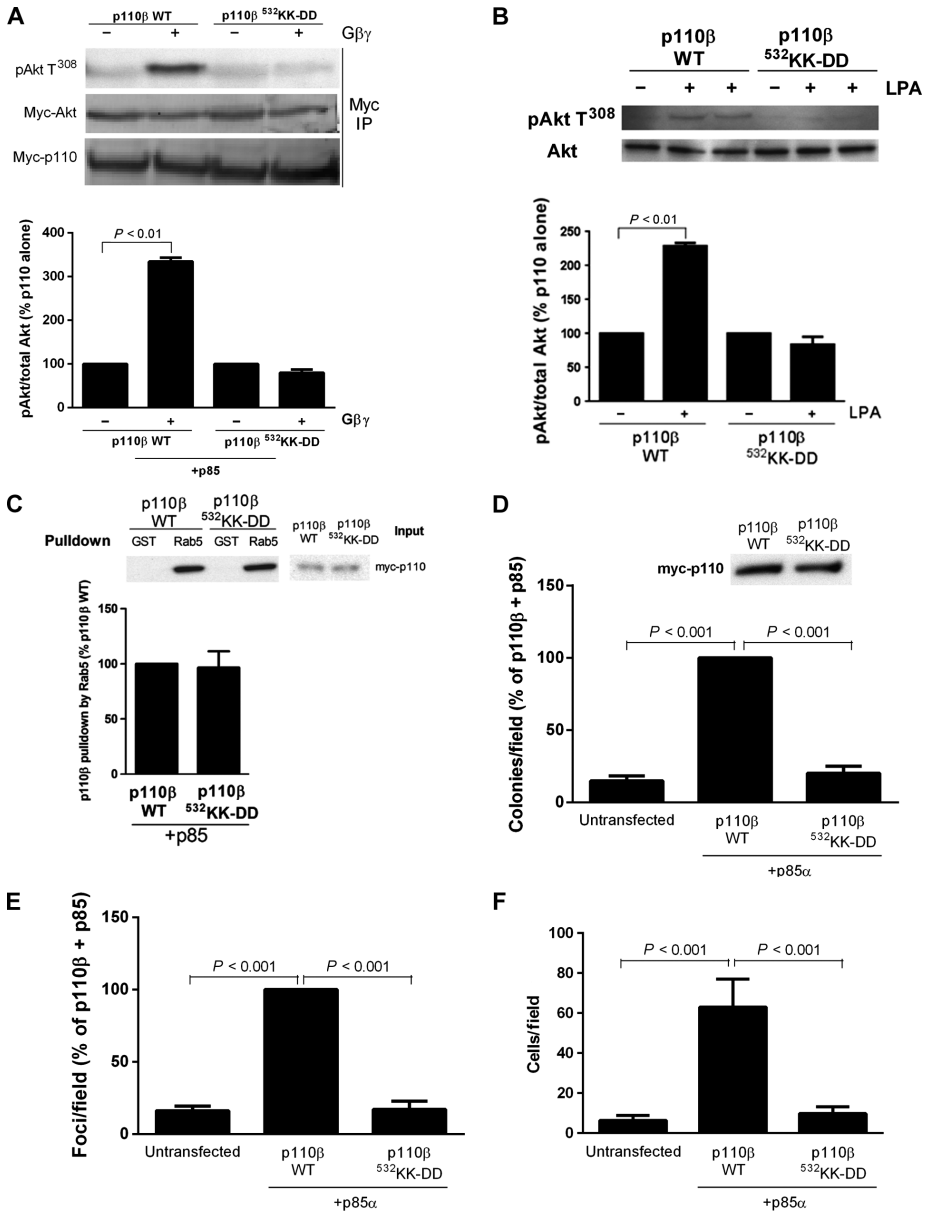

Fig. 2. Role of Gβγ in PI3Kβ-mediated signaling, transformation, motility, and chemotaxis. (**A**) HEK 293E cells were transfected with plasmids encoding myc-Akt and either WT or the ^{532}KK-DD mutant PI3Kβ, with or without plasmids encoding Gβγ. Akt activation in samples immunoprecipitated (IP) with an antibody against myc was analyzed by Western blotting with an antibody against pT^{308}-Akt. The ratio of the amount of pAkt to that of total Akt is expressed as a percentage of that under basal conditions. (**B**) NIH 3T3 cells stably expressing WT or mutant PI3Kβ were stimulated with 10 nM LPA for 5 min. Akt activation was analyzed by Western blotting with anti-pT^{308}-Akt antibody and quantified as described earlier. (**C**) HEK 293T cells were transfected with plasmid encoding WT or ^{532}KK-DD mutant p110β. Cell lysates were incubated with glutathione *S*-transferase (GST) or GST-Rab5 immobilized on glutathione-Sepharose beads, and bound material was analyzed by Western blotting. Graphs in each panel show the mean percentage pulldown ± SEM from three separate experiments. (**D** and **E**) NIH 3T3 cells were transfected with plasmids encoding p85α and either WT or the ^{532}KK-DD mutant p110β, and (D) the formation of colonies in soft agar or (E) the formation of foci were measured. Graphs in each panel show the means ± SEM from three separate experiments. (**F**) Migration of control NIH 3T3 cells or cells stably expressing WT or mutant PI3Kβ toward fetal bovine serum (FBS) was measured in a Boyden chamber assay. Assays were conducted in triplicate, and the data are pooled from two separate experiments.

of Akt activation in the presence of Gβγ subunits (Fig. 2A). Similarly, lysophosphatidic acid (LPA)–stimulated Akt activation was greater in NIH 3T3 cells stably expressing wild-type PI3Kβ than in cells expressing the ^{532}KK-DD mutant p110β (Fig. 2B). The ^{532}KK-DD mutation had no effect on the binding of p110β to the small guanosine triphosphatase (GTPase) Rab5 (Fig. 2C), indicating that interactions of mutant p110β with other intracellular regulators were intact. These data show that the C2-helical linker region of p110β is necessary for Gβγ-mediated activation of PI3Kβ in vitro and in cells.

To test the biological relevance of Gβγ-mediated activation in p110β signaling, we compared the ability of wild-type and mutant p110β constructs to mediate cellular transformation and motility. In a soft-agar colony formation assay, cells transfected with plasmid encoding wild-type PI3Kβ generated substantially more colonies than did control cells. However, transfection of cells with plasmid encoding the ^{532}KK-DD mutant PI3Kβ resulted in a complete loss of transformation (Fig. 2D and fig. S5B). Similar results were obtained in a focus formation assay, in which NIH 3T3 cells transfected with plasmid encoding wild-type PI3Kβ formed a substantially greater number of foci compared to that formed by cells transfected with plasmid encoding the ^{532}KK-DD mutant PI3Kβ (Fig. 2E and fig. S5C). This result was not due to differences in proliferation because wild-type and mutant p110β caused similar increases in proliferation compared to that of control NIH 3T3 cells (fig. S6A). Similarly, wild-type, but not mutant, p110β increased the extent of chemotaxis

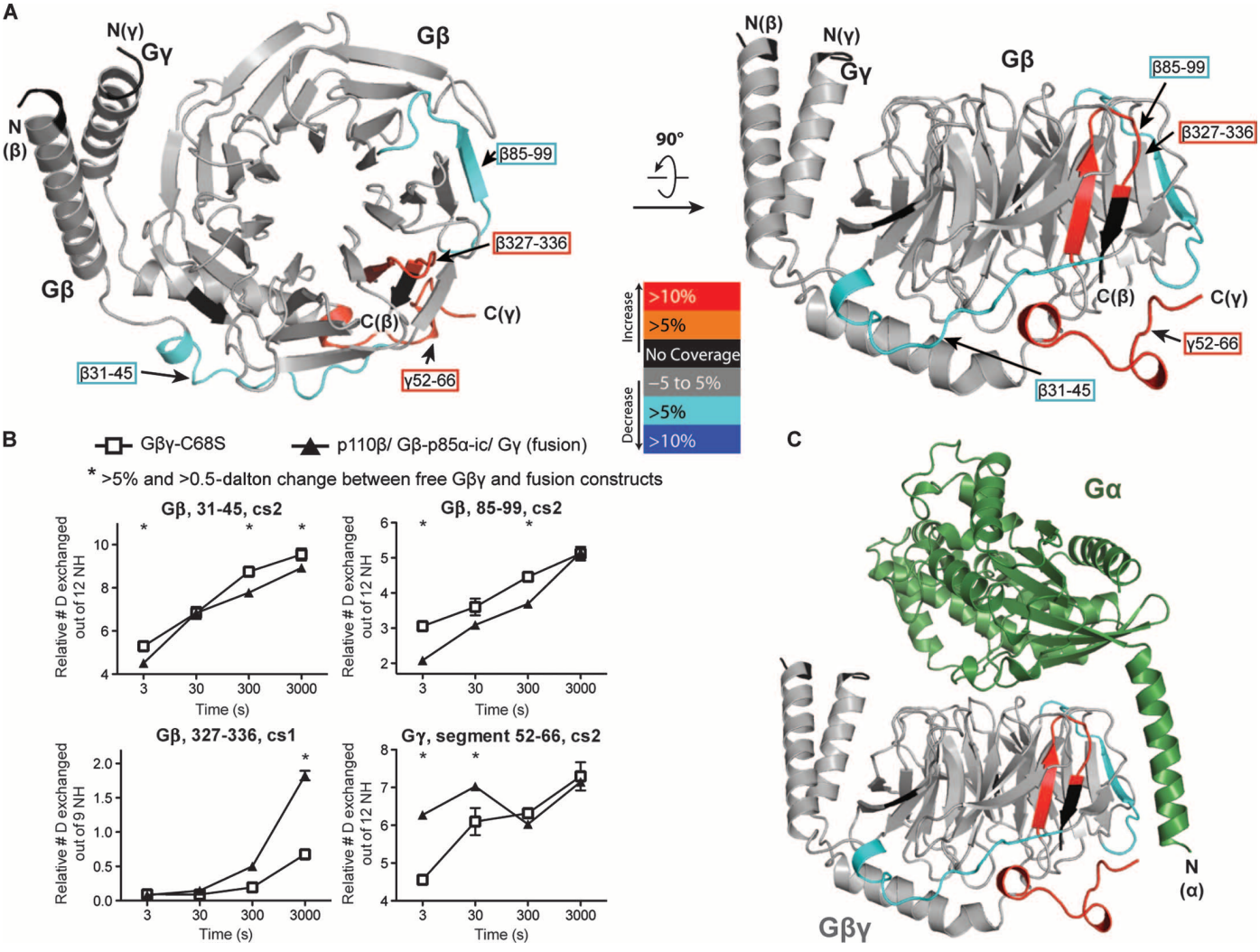

Fig. 3. Mapping of the p110β-binding region in Gβγ heterodimers with HDX-MS. (**A**) The p110β–Gβ-p85α-icSH2–Gγ-C68S fusion heterotrimer (fusion) was used to compare deuterium incorporation with that of free Gβγ-C68S (Gβγ). Regions in Gβ and Gγ that showed >0.5 dalton and >5% changes between free Gβγ and the fusion were mapped onto the Gβγ model (PDB ID: 1GOT). In addition to the protected peptides described in the text, there was some exposure of the C terminus of Gβ and the adjacent C terminus of Gγ, which were probably a consequence of the attachment of the C terminus of Gβ to the linker connecting to p85 in the fusion. (**B**) All peptides in Gβ and Gγ that showed changes in deuteration extent between free Gβγ and the fusion proteins are shown. The stretch of amino acid residues 52 to 66 in Gγ is labeled as a segment to denote that these data were generated by subtraction of the deuterium incorporation of peptides 44 to 51 from that of peptides 44 to 66. Stars indicate changes that were >0.5 dalton and >5%. Experiments were performed in duplicate and graphs show the SD. (**C**) Crystal structure of Gβγ bound to Gα (PDB ID:1GOT). Gβγ is colored as in (A).

of cells toward serum in a Boyden chamber assay (Fig. 2F). The ability of wild-type p110β to enhance transformation and migration was Gβγ-dependent because it was inhibited by pertussis toxin (fig. S6, B and C). These data showed that the GPCR inputs to PI3Kβ transmitted by Gβγ are critical for PI3Kβ-mediated cellular transformation and enhancement of motility.

Identification of the p110β-binding site on Gβγ by HDX-MS

To explore the possibility of specifically inhibiting the interactions between p110β and Gβγ, we used the HDX-MS approach to determine the region on Gβγ that binds to p110β (Fig. 3). We identified two regions on Gβγ that were more protected in the fusion compared to in the free Gβγ. One of the peptides spans residues 31 to 45 in Gβ, in the linker between the N-terminal α-helix and the first blade of the β-propeller (Fig. 3, A and B). This region was not previously observed to interact with other Gβγ effectors. The other more protected stretch spans residues 85 to 99 in the second blade of the β-propeller, a region previously identified to be of major importance for the activation of phospholipase C β2 (PLC-β2) (*23*, *24*). This region contains the residue Trp^{99} at the top of the propeller, which is part of the "hotspot" region in Gβ that makes contacts with several effectors (*25*). These data showed that p110β shares a common Gβγ-binding surface with other effectors, such as the G protein α-subunit (Fig. 3C), PLC-β, adenylyl cyclase (*26*), and PI3Kγ (*27*), but that it also uniquely affects a linker region between the N-terminal α-helix and the first blade of Gβ. This interface could provide an attractive target for therapeutics because targeted disruption of this interface should have relatively specific effects on Gβγ-mediated activation of p110β.

Inhibition of the proliferation, chemotaxis, and invasion of PTEN-null tumor cells by a peptide inhibitor of the p110β-Gβγ interaction

To generate an inhibitor of p110β-Gβγ interactions, we synthesized a peptide derived from the C2-helical linker region of p110β (^{514}KAAEIASSDSANVSSRGGKKFLPV). The peptide had no effect on basal PI3Kβ activity (Fig. 4A) but blocked Gβγ-dependent activation of PI3Kβ in vitro, whereas a scrambled peptide had no effect (Fig. 4B). Similar results were obtained with N-myristoylated and N–HIV-1 trans-acting transcriptional activator (TAT)–labeled versions of the peptide (Fig. 4C), which are cell-permeable versions of the peptide. The peptide had no effect on Gβγ-mediated activation of p101-p110γ dimers, which were inhibited by peptides that target the canonical Gβγ effector–binding site (SIGK and QEHA, Fig. 4D).

We tested the effects of the myristoylated peptide on Gβγ-mediated activation of Akt in NIH 3T3 cells transfected with plasmid encoding myc-Akt with or without plasmids encoding Gβγ subunits. The myristoylated p110β peptide completely inhibited Gβγ-mediated (Fig. 5A) and LPA-stimulated (Fig. 5B) increases in Akt phosphorylation at Thr^{308} at a concentration of 30 μM (fig. S7A), whereas myristoylated scrambled peptide or vehicle control had minimal effects. In contrast, the myristoylated peptide had no effect on epidermal growth factor–dependent activation of Akt in a cell line in which TGX221 had a substantial inhibitory effect (fig. S7B), which showed that the myristoylated peptide had no effect on RTK-mediated activation of PI3Kβ in intact cells. The inhibitory activity of the myristoylated peptide required its entry into the cells because both myristoylated and TAT-tagged peptides inhibited Gβγ-dependent activation of Akt, whereas unmodified peptide had no such effect (fig. S7C). In addition, the myristoylated p110β peptide, but not the myristoylated scrambled peptide, inhibited PI3Kβ-dependent transformation of NIH 3T3 cells, as was observed in a soft-agar colony formation assays (Fig. 5C and fig. S5B) and focus formation assays (Fig. 5D and fig. S5C). Inhibition of cellular transformation by the myristoylated p110β peptide was not a result of decreased proliferation because neither the myristoylated peptide nor pertussis toxin inhibited the proliferation of NIH 3T3 cells transfected with plasmid encoding PI3Kβ (fig. S7D). In contrast, the myristoylated peptide had no effect on cellular transformation caused by expression of oncogenic Ras (Fig. 5E). The myristoylated peptide also blocked

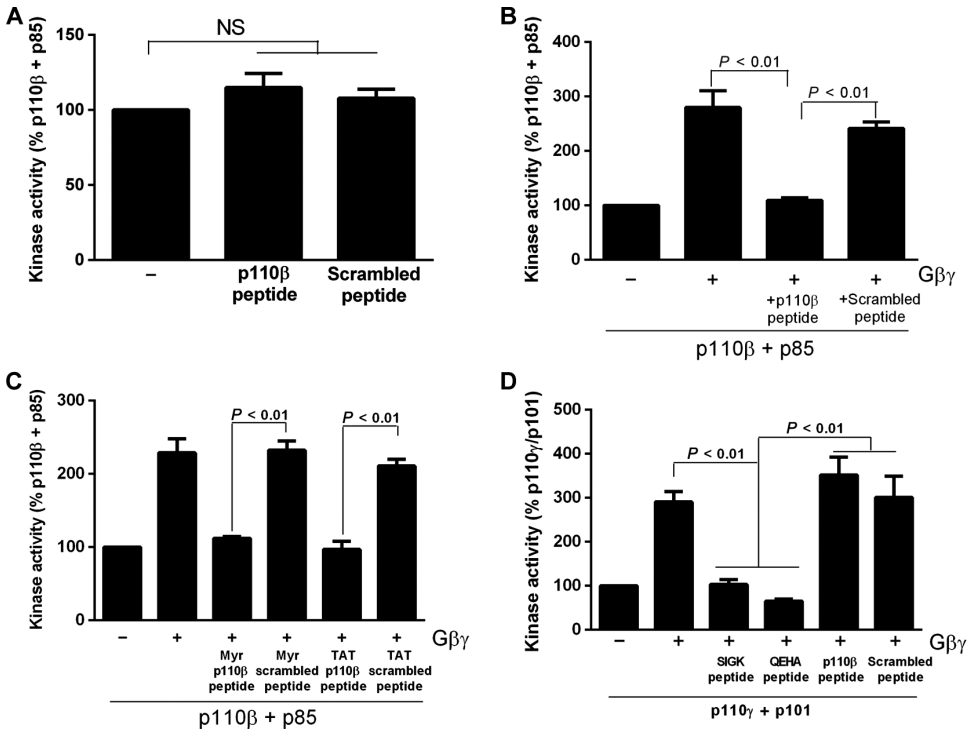

Fig. 4. A peptide derived from p110β blocks the activation of PI3Kβ by Gβγ in vitro. (**A**) PI3Kβ immunopurified from HEK 293T cells was incubated in the absence or presence of 1 μM p110β peptide or scrambled peptide and assayed for lipid kinase activity. (**B**) PI3Kβ immunopurified from HEK 293T cells was incubated in the absence or presence of recombinant lipidated Gβγ and 1 μM p110β peptide or scrambled peptide and assayed for lipid kinase activity. (**C**) PI3Kβ immunopurified from HEK 293T cells was incubated in the absence or presence of recombinant lipidated Gβγ and 1 μM myristoylated or TAT-tagged p110β peptide or scrambled peptide and assayed for lipid kinase activity. (**D**) Immunopurified p101-p110γ from HEK 293T cells was incubated with or without recombinant lipidated Gβγ and 1 μM p110β peptide, scrambled peptide, 1 μM QEHA peptide, or 10 μM SIGK peptide. Data are the means ± SEM of triplicate measurements and are representative of two to three experiments.

the enhanced migration in a Boyden chamber assay of NIH 3T3 cells transfected with plasmid encoding PI3Kβ (Fig. 5F).

Control experiments showed that the effects of the myristoylated peptide were specific for p110β-Gβγ interactions. The myristoylated peptide did not reduce the abundance of p110β protein (Fig. 5, C and D). In addition, the myristoylated p110β peptide had no effect on Gβγ-dependent activation of the class IB PI3K (the p101-p110γ dimer) (fig. S8A), the synergistic activation of adenylyl cyclase by Gβγ and Gαs (fig. S8B), or the Gβγ-mediated activation of PLC-β in cells (fig. S8C), and the non-modified peptide had no effect on Gβγ-mediated activation of PLC-β in vitro (fig. S8D). Similarly, the myristoylated peptide had no effect on the p110β-dependent induction of autophagy or the binding of p110β to Rab5 (fig. S8, E and F) (*28*), which is in agreement with the ^{532}KK-DD mutant p110β having no effect on Rab5 binding (Fig. 2C). Thus, the effects of the myristoylated peptide specifically disrupted p110β-Gβγ interactions. These data showed that p110β-mediated cellular transformation and migration requires the binding of p110β to Gβγ.

The growth of PTEN-null tumors depends on p110β (*8*), and inhibition of Gβγ signaling or knock-in of a kinase-deficient p110β blocks the growth of prostate cancer cells (*9*, *29*). To test the role of p110β-Gβγ interactions in PTEN-null prostate cancer cells, we measured the proliferation of PC-3 cells in the presence of myristoylated p110β peptide or scrambled peptide. Whereas PC-3 cell proliferation was unaffected by the myristoylated scrambled peptide or by the p110β inhibitor TGX221, proliferation was inhibited in the presence of myristoylated p110β peptide or pertussis toxin (Fig. 6A). Similar effects were seen in the PTEN-null endometrial cancer cell lines AN3CA and RL95-2 but not in the PTEN-replete endometrial cancer line KLE (Fig. 6B). Myristoylated p110β peptide also inhibited the chemotaxis of PC-3 cells toward serum in a Boyden chamber assay (Fig. 6C). Finally, in a collagen invasion assay designed to mimic paracrine interactions between macrophages and tumor cells during invasion (*30*), macrophage-dependent PC-3 cell invasion was blocked by the myristoylated p110β peptide (Fig. 6D) but not by myristoylated scrambled peptide. These data suggest that GPCR-mediated activation of p110β in PTEN-null cells plays a critical role in proliferation, chemotaxis, and paracrine interactions between tumor cells and macrophages during invasion.

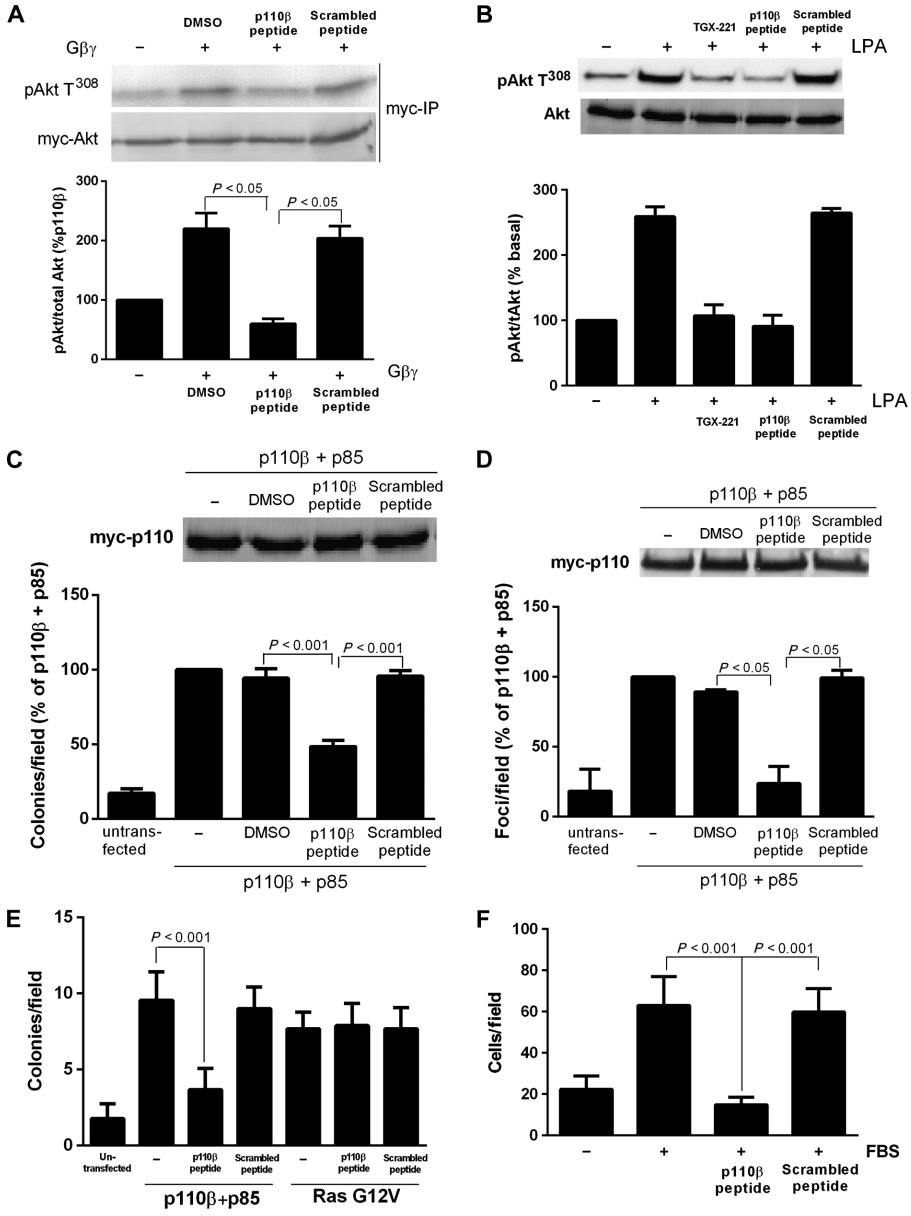

Fig. 5. Peptide inhibitors disrupt PI3Kβ activation and signaling in response to Gβγ. (**A**) HEK 293E cells were transfected with plasmids encoding p110β, p85, and myc-Akt with or without plasmid encoding Gβγ. Cells were treated with 30 μM peptide or scrambled peptide for 30 min, and the extent of phosphorylation of Akt at Thr^{308} (T^{308}) was determined by Western blotting analysis. (**B**) NIH 3T3 cells were pretreated with TGX221, p110β peptide, or scrambled peptide and stimulated with 10 nM LPA for 5 min before the extent of phosphorylation of Akt at Thr^{308} was determined by Western blotting analysis. (**C**) NIH 3T3 cells were transfected with plasmids encoding WT p110β and p85α, and colony formation in soft agar was measured in the absence or presence of 30 μM p110β-derived myristoylated peptide or scrambled peptide. (**D**) NIH 3T3 cells were transfected with plasmids encoding WT p110β and p85α, and the formation of foci was measured in the absence or presence of 30 μM p110β-derived myristoylated peptide or scrambled peptide. (**E**) NIH 3T3 cells were transfected with plasmids encoding p110β and p85 or with plasmid encoding ^{12}V-Ras. Cells were incubated with or without p110β peptide or scrambled peptide, and the formation of colonies in soft agar was measured. (**F**) Migration of NIH 3T3 stably expressing p110β and p85α toward FBS in a Boyden chamber, in the absence or presence of p110β peptide or scrambled peptide. The graphs in panels (A) to (D) and (F) show the means ± SEM from three to four separate experiments. The data in (E) show the means ± SEM from triplicate measurements and are representative of two experiments.

DISCUSSION

Over the last few years, there has been an increased appreciation of the roles of GPCRs in cancer, both through direct signaling and by transactivation of RTKs (*31*–*33*). Although the activation of the PI3Kβ isoform of PI3K by Gβγ subunits has been known for many years, the mechanism of this interaction is unclear, and it has been difficult to specifically study GPCR-regulated signaling by PI3Kβ. Our identification of the Gβγ-binding site in p110β and the reciprocal p110β-binding site in Gβγ has enabled the construction of mutants and peptide-based inhibitors that specifically disrupt this interaction. Using these approaches, we have demonstrated a critical role for Gβγ signaling to PI3Kβ in p110β-mediated transformation, as well as in the proliferation and invasion of PTEN-null prostate cancer cells. Our data suggest that GPCR-mediated activation of PI3Kβ could provide a new target for the design of anticancer therapeutics.

The Gβγ-binding site comprises a surface loop that bridges helices Lα5 and H1A between the C2 and helical domains of p110β. This loop is close to the inhibitory contact site for the nSH2 domain of p85 (Glu^{552}). We can propose two mechanisms for the activation of p110β by Gβγ: one through membrane recruitment and the other through relief of SH2-mediated inhibition. These mechanisms are not mutually exclusive, and it is likely that both contribute. Gβγ stimulates p110β in the absence of p85 (*7*), as well as when p110β was associated with a p85 construct consisting of only the iSH2 domain (p85-i) or with a construct having the iSH2 connected to the inhibitory cSH2 domain (p85-ic) (fig. S9). Furthermore, Gβγ activated PI3Kβ in the absence of pY (Fig. 1F). Consequently, relief of SH2-mediated inhibition cannot be the only mechanism of activation of p110β by Gβγ. Our studies with PI3Kβ and Gβγ in the presence of liposomes showed that Gβγ binding enhanced the interactions of the kinase domain with lipid membranes (fig. S2, B and D). This suggests that a portion of the activation mechanism involves increased targeting to membranes because of the lipid moiety of the prenylated Gβγ. On the other hand, activation of p110β by pY peptides involves the relief of inhibition by the N- and C-terminal SH2 domains (*15*), and both pY and Gβγ are required for maximal stimulation of PI3Kβ. It is possible that pY binding to the nSH2 only partially relieves its inhibitory contact and that Gβγ more completely displaces it to achieve full activation. It is also possible that by Gβγ increasing the membrane affinity, the presence of the membrane surface sterically helps to displace the inhibitory N- and C-terminal SH2 domains. Of note, the Gβγ-binding region of p110β shows low sequence similarity with the corresponding region of the other Gβγ-regulated PI3K catalytic subunit, p110γ. Consequently, it is not straightforward to predict the Gβγ-binding region of p110γ, and this will require experimental mapping.

Because the peptide inhibitor did not affect the activity of p110β directly, we presume that its mechanism of action is through binding to the p110β-interacting site within Gβγ. HDX-MS analysis of p110β binding to Gβγ revealed a partial overlap with surfaces that bind to canonical Gβγ effectors, as well as a region that appears to be unique to p110β: the linker region between the N-terminal α-helix and the first blade of Gβ. We have not determined the binding site for the p110β-derived peptide within Gβγ. However, the specificity of the peptide's effects for the interaction between Gβγ and p110β, rather than adenylyl cyclase, PLC-β, or p101-p110γ, suggests that the peptide interacts with the unique region of the p110β-binding surface in Gβγ. An alternative explanation accommodates the fact that the binding of p110β to Gβγ is weak relative to that of other canonical effectors. In this model, the p110β peptide may bind to a portion of the canonical interface, but with

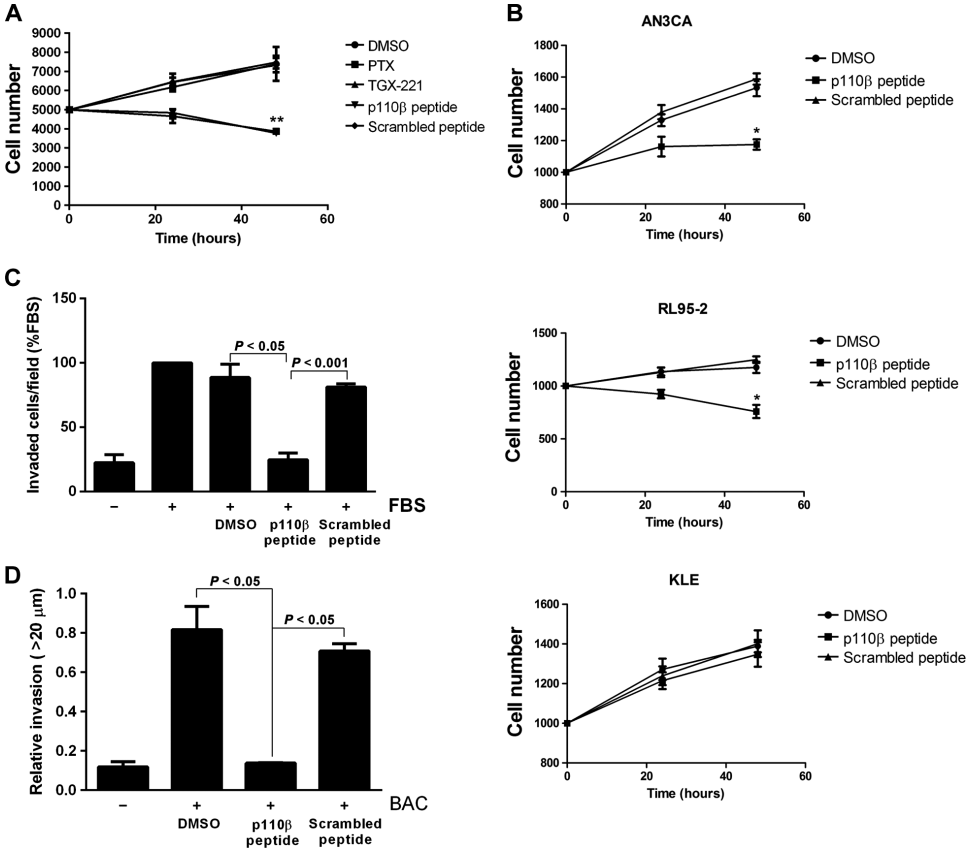

Fig. 6. Inhibition of the proliferation and chemotaxis of prostate cancer cells. (**A**) The proliferation of PC-3 cells was measured by the MTT assay in the absence or presence of 200 nM TGX221, 30 μM myristoylated p110β-derived peptide, or 30 μM scrambled peptide. (**B**) Proliferation assays were performed on two PTEN-null endometrial cancer cell lines (AN3CA and RL95-2 cells) and one PTEN-positive endometrial cancer cell line (KLE cells) grown in the absence or presence of myristoylated p110β-derived peptide or scrambled peptide. (**C**) Chemotaxis of PC-3 cells toward 10% FBS in the absence or presence of 20 μM p110β-derived peptide or scrambled peptide was measured in Boyden chambers. (**D**) Bone marrow–derived macrophages and CellTracker Red–labeled PC-3 tumor cells were coplated in 24-well dishes and overlaid with collagen. Cells were incubated for 24 hours in the absence or presence of p110β-derived peptide or scrambled peptide, and invasion into the collagen was measured by confocal microscopy. Data are the means ± SD from two separate experiments for (B) and (D) and are the means ± SEM from three separate experiments for (A) and (C).

an affinity low enough to displace p110β but not other Gβγ effectors. We cannot experimentally distinguish between these hypotheses at this time. Finally, it is formally possible that the peptide contacts Gβγ in a manner that is distinct from that which occurs with the corresponding loop in p110β. Studies are in progress to define the peptide-binding site, and these will be useful in designing a better inhibitor of the Gβγ-p110β interaction.

PI3Kβ is ubiquitously expressed and has been implicated in the regulation of vascular tone (*34*), thrombogenesis (*35*), male fertility (*36*), phagocytosis in macrophages (*37*), and integrin signaling (*38*). In addition, p110β has kinase-independent functions, including involvement in clathrin-mediated endocytosis, cell proliferation, and DNA repair (*10*, *39*, *40*). The role of GPCR signaling to PI3Kβ in these systems can now be directly addressed. With regard to the requirement for PI3Kβ in PTEN-null tumors (*8*), our data suggest that Gβγ interactions with PI3Kβ are critical for the growth and invasion of these tumors. Surprisingly, the peptide was more efficacious in inhibiting the proliferation of PC-3 cells than was the p110β-specific kinase inhibitor TGX221. This is consistent with studies showing that kinase-deficient p110β rescues proliferative defects in mice (*10*, *39*) and suggests that at least some of the Gβγ signaling to p110β involves the scaffolding functions of p110β. In contrast, previous studies have shown that kinase-deficient p110β does not support transformation in PTEN-null cells (*8*), suggesting that stimulation of PI3Kβ activity by Gβγ is required for transformation.

The role of GPCR signaling in PTEN-null tumors has not been extensively studied. It will be important to determine whether peptidomimetics or other small-molecule inhibitors of the p110β-Gβγ interface might be therapeutically useful in the treatment of some PTEN-null tumors. Currently, we do not know which GPCRs function upstream of Gβγ in the activation or targeting, or both, of PI3Kβ. Defining these upstream inputs would provide an alternative approach to the treatment of tumors dependent on p110β.

MATERIALS AND METHODS

Design and cloning of constructs and transfections

The loop swap, ^{532}KK-DD and ^{514}KAAEI-DAAKA mutants were generated with the QuickChange kit (Stratagene). The Gβ-p85α-icSH2 fusion construct was cloned with standard digestion and ligation strategies, linking the sequence encoding the C terminus of human $Gβ_1$ to that encoding the N terminus of human p85α-ic (residues 432 to 724) with a 25-residue linker of the following sequence: GSPGISGGGGGPGSGGGGSGGGGSG. All mutants were confirmed by sequencing. Transfections were performed with FuGENE HD (Roche).

Purification of p110β-p85α dimers expressed in insect cells

Recombinant baculoviruses were generated and propagated with the Bac-to-Bac expression system (Invitrogen) according to the manufacturer's recommendations. For expression, 3 liters of *Spodoptera frugiperda* (Sf9) cells at a density of 1.0×10^6 cells/ml were co-infected with an optimized ratio of viruses encoding complexes of the catalytic and regulatory subunit of PI3K. After 55 hours of infection at 27°C, cells were harvested and washed with ice-cold phosphate-buffered saline (PBS) supplemented with 0.5 mM 4-(2-aminoethyl) benzenesulfonyl fluoride hydrochloride (AEBSF; Melford). Subsequently, cells were lysed by sonication for 4 min in 120 ml of buffer A1 [20 mM tris (pH 8), 300 mM NaCl, 10 mM imidazole] containing 0.5 mM AEBSF and were centrifuged for 20 min at 140,000*g*. The supernatant was filtered through a 0.45-μm Minisart filter unit (Sartorius Biotech) before loading onto two connected 5-ml HisTrap FF columns (GE Healthcare). The columns were washed first with buffer A1 and then with buffer A2 [20 mM tris (pH 8), 100 mM NaCl, 10 mM imidazole, 2 mM 2-mercaptoethanol (2-ME)] and eluted with a gradient from 0 to 100% of buffer A2 containing 150 mM imidazole. Fractions were analyzed on 4 to 12% bis-tris Novex gels (Invitrogen) with Mops buffer. The protein complex was further purified on a 5-ml HiTrap Q-HP column (GE Healthcare) with buffer C [20 mM tris (pH 8), 2 mM dithiothreitol (DTT)] and was eluted with buffer D [20 mM tris (pH 8), 2 mM DTT, 1 M NaCl]. The complex was concentrated with Amicon 50K centrifugal filters (Millipore) and loaded onto a 16/60 Superdex 200 gel filtration column (GE Healthcare) at 4°C running with buffer E [20 mM Hepes (pH 7.5), 100 mM NaCl, 2 mM tris(2-carboxyethyl)phosphine (TCEP)]. The heterodimer was concentrated to about 5 mg/ml, frozen in liquid nitrogen, and stored at −80°C.

Purification of p110β-p85α dimers from mammalian cells

HEK 293T cells were cotransfected with plasmids encoding myc-p110β and p85α, and the proteins were coimmunoprecipitated with anti-myc antibody. Pellets were washed sequentially three times in PBS containing 1% NP40; three times in 50 mM tris (pH 7.4) and 500 mM $LiCl_2$; and twice in 20 mM tris (pH 7.5), 100 mM NaCl, and 1 mM EDTA. Pellets were resuspended in a final volume of 50 μl of 40 mM Hepes (pH 7.4), 0.1% bovine serum albumin (BSA), 1 mM EGTA, 7 mM $MgCl_2$, 120 mM NaCl, 1 mM DTT, and 1 mM β-glycerophosphate.

Purification of Gβγ expressed in insect cells

Recombinant human $Gβ_1$, N-terminally hexahistidine-tagged bovine wild-type $Gγ_2$, and the $Gγ_2$(C68S) mutant were produced in Sf9 cells and purified as described previously (*27*). Isoprenylated $Gβ_1$His-γ2 was isolated from the membrane fraction. The membrane extract was clarified by ultracentrifugation at 100,000*g* for 1 hour and diluted five times with a buffer containing 20 mM Hepes-NaOH (pH 7.7), 100 mM NaCl, 0.1% polyoxyethylene-10-lauryl ether (C12E10), and 10 mM 2-ME. The extract was supplemented with 25 mM imidazole and incubated with Ni^{2+}-NTA Superflow beads (Qiagen) for 1 hour. The mixture was loaded onto a column cartridge and extensively washed with buffer containing 20 mM imidazole. Thereafter, bound insect Gα subunits were eluted with $AlCl_3$ in the presence of Mg^{2+}. Subsequently, $Gβ_1$His-γ2 dimers were eluted with a buffer containing 20 mM tris-HCl (pH 8.0), 25 mM NaCl, 0.1% C12E10, 200 mM imidazole, and 10 mM 2-ME. $Gβ_1$His-γ2 eluted from the Ni^{2+}-NTA matrix was diluted and loaded onto a 1-ml Resource 15Q HR 5/5 column (GE Healthcare) equilibrated with a buffer containing 20 mM tris-HCl (pH 8.0), 8 mM CHAPS, and 2 mM DTT. Bound proteins were eluted and fractionated with a continuous gradient elution (0 to 500 mM NaCl). Peak fractions were pooled and concentrated with Amicon 10 concentrators (Millipore). The protein was then loaded onto a gel filtration Superdex 200 HR 10/30 column (GE Healthcare) and eluted with a buffer containing 20 mM Hepes-NaOH (pH 7.7), 100 mM NaCl, 10 mM CHAPS, and 2 mM TCEP. Peak fractions were pooled and concentrated with Amicon 10 concentrators (Millipore). Purified proteins were quantified by Coomassie Brilliant Blue staining after SDS–polyacrylamide gel electrophoresis (SDS-PAGE) analysis with BSA as a standard. Proteins were stored at −80°C. Nonlipidated $Gβ_1$His-γ2(C68S) was purified from the cytosolic fraction of Sf9 cells. After separation from the membrane fraction, the cytosolic fraction was supplemented with 15 mM imidazole and incubated with Ni^{2+}-NTA Superflow beads (Qiagen) for 1 hour. The mixture was loaded onto a column cartridge and extensively washed with a buffer containing 20 mM Hepes-NaOH (pH 7.7), 300 mM NaCl, 15 mM imidazole, and 10 mM 2-ME. $Gβ_1$His-γ2(C68S) mutants were eluted with a buffer containing 20 mM tris-HCl (pH 8.0), 25 mM NaCl, 200 mM imidazole, and 10 mM 2-ME. The protein eluted from the Ni^{2+}-NTA matrix

was diluted and loaded onto a 1-ml Resource 15Q HR 5/5 column (GE Healthcare) equilibrated with a buffer containing 20 mM tris-HCl (pH 8.0) and 2 mM DTT. Bound proteins were eluted and fractionated with a continuous NaCl gradient elution (0 to 600 mM NaCl). Peak fractions were pooled and concentrated with Amicon 10 concentrators (Millipore). The protein was then loaded onto a gel filtration Superdex 200 HR 10/30 column (GE Healthcare) and eluted with a buffer containing 20 mM Hepes-NaOH (pH 7.7), 100 mM NaCl, and 2 mM TCEP. Peak fractions were pooled and concentrated with Amicon 10 concentrators (Millipore). Purified proteins were quantified by Coomassie Brilliant Blue staining after SDS-PAGE with BSA as a standard. Proteins were stored at −80°C.

Preparation of lipid vesicles

For assays with immunopurified material from mammalian cells, lipid vesicles consisting of 38% phosphatidylethanolamine (PE), 35.5% phosphatidylserine (PS), 16.3% phosphatidylcholine (PC), 3.5% sphingomyelin, and 6.7% phosphatidylinositol-4,5-bisphosphate (PIP_2) (all percentages by weight) (*41*) were dried under argon; resuspended at 0.66 μg/μl in 40 mM Hepes (pH 7.4), 0.1% BSA, 1 mM EGTA, 7 mM $MgCl_2$, 120 mM NaCl, 1 mM DTT, and 1 mM β-glycerophosphate; and sonicated in a Branson cup sonicator. For assays with recombinant protein purified from insect cells, vesicles were prepared by adding the lipid components together in chloroform and evaporating the organic solvent under a stream of dry argon. The lipid film was allowed to dry for 30 min under vacuum and was then resuspended in a solution of 20 mM tris (pH 7.5), 100 mM KCl, and 1 mM EGTA. The lipids were first bath-sonicated for 10 min and then subjected to 10 cycles of freeze-thaw between liquid nitrogen and a 37°C water bath. The liposomes were finally extruded 10 times through a 100-nm filter (Whatman, Anotop 10) with a gas-tight syringe. Vesicles were frozen at −80°C for storage and were used within 1 month of preparation. Vesicle composition was 5% brain-PIP_2 (Sigma), 20% brain-PS (Sigma), 45% brain-PE (Avanti), 15% dioleoyl-PC (Avanti), 10% cholesterol (Sigma), and 5% egg-sphingomyelin (Sigma). Percentages are based on weight.

Assay of lipid kinase activity with immunopurified enzyme

For assays with immunoprecipitated enzymes, myc-tagged wild-type or mutant p110β together with p85α was coimmunoprecipitated with an anti-myc antibody from appropriately transfected HEK 293T cells. For assays with Gβγ, Gβγ was preincubated with lipid vesicles for 30 min and then added to the resuspended enzyme pellets (*41*). For assays with phosphopeptide, 1 μM (final concentration) tyrosyl phosphorylated peptide [mouse PDGFR residues 735 to 767, sequence: ESDGG(pY)MDMSKDESID (pY)VPMLDMKGDIKYADIE; referred to as pY] and lipid vesicles were added directly. The assay (immunoprecipitated enzyme and 200 nM Gβγ, 320 μM PE, 300 μM PS, 140 μM PC, 30 μM Sphingomyelin, and 300 μM PI in a final volume of 81 μl) was initiated by the addition of 5 μl of adenosine 5′-triphosphate (ATP) (116 μM final concentration) containing 1 μCi of [^{32}P]ATP. After 10 min at 22°C, the assay was stopped by the addition of EDTA (50 μM final concentration), and 5-μl aliquots were spotted on nitrocellulose membranes. The membranes were washed five times in 1 M NaCl containing 1% phosphoric acid, dried, and counted with a Molecular Dynamics PhosphorImager. Alternatively, assays were analyzed by thin layer chromatography by stopping the reaction with 20 μl of 8N HCl, mixing with 160 μl of a 1:1 solution of methanol/chloroform, and centrifugation to separate the phases; after which, 20 μl of the organic phase was spotted onto a silica gel plate (EMD Merck). Plates were developed in a solvent system consisting of 60 ml of chloroform, 47 ml of methanol, 11.2 ml water, and 2 ml of ammonium hydroxide; dried; and counted with a Molecular Dynamics PhosphorImager. For assays using the inhibitory peptides, a 1 μM final concentration of peptides (wild-type p110β: KAAEIASSDSANVSSRGGKKFLPV; scrambled p110β: NGAEKVGSADSKSIAFVSLKARSP) in 20 mM tris-HCl (pH 7.4) and 10 mM NaCl was incubated with 200 nM Gβγ for 30 min on ice, and then with lipids, as described earlier, for 10 min on ice, and finally for 10 min with immunopurified PI3K; after which, the kinase assay described earlier was performed. For assays of immunopurified PI3Kγ in the presence of peptide, peptides (1 μM wild-type p110β; 1 μM scrambled p110β; 10 μM SIGK: SIGKAFKILGYPDYD; or 1 μM QEHA: QEHAQEPERQYMHIGTMVEFAYALVGK) in 20 mM tris-HCl (pH 7.4) and 10 mM NaCl were incubated with 200 nM Gβγ for 30 min on ice and then incubated with lipids as described earlier for 10 min on ice, before finally being incubated for 10 min with immunopurified PI3Kγ from baculovirus-infected insect cells; after which, the kinase assay described above was performed.

Assay of lipid kinase activity with enzyme purified from insect cells

For assays with recombinant PI3K from baculovirus-infected insect cells, lipid vesicles were used at a final concentration of 1 mg/ml and were prepared as described earlier. Stock solutions of threefold concentrated wild-type or mutant PI3Kβ constructs were prepared at 75 nM (for assays of basal, pY-stimulated, and Gβγ-stimulated activity) and at 0.75 nM (for assay of synergistic activation by pY and Gβγ) in 20 mM Hepes (pH 7.5), 100 mM NaCl, 2 mM DTT, 9 mM $MgCl_2$, and 3 mM EDTA. Substrate stock solutions containing lipids (3 mg/ml) supplemented with either 900 nM RTK-pY [from a 100 μM stock in 10 mM Hepes (pH 7.5), 0.2% dimethyl sulfoxide (DMSO)], 1.5 μM $G\beta_1\gamma_2$ [from a 50 μM stock in 20 mM Hepes (pH 7.5), 100 mM NaCl, 2 mM TCEP, 10 mM CHAPS], or both agonists were prepared in 20 mM Hepes (pH 7.5), 100 mM NaCl, and 2 mM DTT. The concentrations of CHAPS and DMSO were adjusted to be equal under all conditions. A 300 μM ATP solution containing [γ^{32}P]ATP (0.1 mCi/ml) was prepared. The reaction was started by mixing 3 μl of protein stock with 3 μl of substrate stock and 3 μl of ATP solution. The reaction was stopped after 60 min by transferring 3 μl of reaction mixture to 3 μl of a 20 mM EDTA quench buffer. Lipid kinase activity was determined with a modified membrane-capture radioactive assay measuring the production of ^{32}P-labeled PIP_3 (*42*). Three microliters of this mixture was then spotted on a nitrocellulose membrane. The membrane was dried and washed six times with 1 M NaCl containing 1% phosphoric acid. The membrane was then air-dried before exposure to a phosphor screen (Molecular Dynamics) for 15 min. The intensity of the spots on the membrane was imaged with a Typhoon PhosphorImager (GE Healthcare) and quantified with ImageQuant software (GE Healthcare).

HDX-MS measurements

HDX-MS analyses of PI3Kβ and Gβγ were performed by following a similar protocol as that previously described (*16*). In the experiment identifying interaction sites between PI3Kβ and soluble Gβγ-C68S, the rate of exchange of the p110β–$G\beta_1$-p85α-icSH2–$G\gamma_2$-C68S fusion heterotrimer was compared to those of a p110β–p85α-icSH2 free heterodimer and a free $G\beta_1\gamma_2$-C68S heterodimer. Protein stock solutions at 7 μM were prepared in 20 mM Hepes (pH 7.5), 100 mM NaCl, and 2 mM DTT. Exchange reactions were started by mixing 10 μl of protein stock with 40 μl of a 98% D_2O solution containing 10 mM Hepes (pH 7.5) and 50 mM NaCl, reaching a final concentration of 78% D_2O. Deuterium exchange reactions were run for 3, 30, 300, and 3000 s of on-exchange at 23°C before the reactions were quenched. An additional experiment for 3 s of on-exchange was performed at 0°C to examine the exchange rates of very rapidly exchanging hydrogens. On-exchange was stopped with 20 μl

of quench buffer containing 1.2% formic acid and 2 M guanidine-HCl, which lowered the pH to 2.6. Samples were then immediately frozen in liquid nitrogen and stored at −80°C for no longer than 7 days. For HDX-MS studies in the presence of lipids, on-exchange experiments were performed in the presence of 10 μM PDGFR pY. Lipid vesicles at 5 mg/ml were diluted eightfold with the 98% D_2O solution described earlier. Protein stock solutions containing 10 μM pY [40 μM stock in 10 mM Hepes (pH 7.2) and 0.08% DMSO] were prepared and incubated for 10 min before the addition of deuterated buffer. To shift the equilibrium toward the PI3Kβ-lipidated Gβγ complex and minimize the concentration of free p110β-p85 heterodimer, we used a Gβγ concentration (10 μM) that was in excess of the PI3Kβ concentration (3 μM). PI3Kβ-pY (state 1), in the presence of lipids (state 2), and in the presence of lipids and Gβγ (state 3) were used in this set of experiments to differentiate between changes in the exchange of PI3Kβ arising from membrane interaction and those from Gβγ interaction. Exchange reactions were started by the addition of 10 μl of protein stock to 40 μl of lipid-containing D_2O solution, reaching a final concentration of 69% D_2O. Deuterium exchange reactions ran for the same time points described for experiments with the fusion construct, but no measurements were performed at 0°C because of problems with lipid precipitation. Samples were stored at −80°C for a maximum of 1 week before deuterium incorporation was measured. Every time point and state was a unique experiment, and every HDX-MS experiment was repeated twice.

Measurement of deuterium incorporation

Samples were rapidly thawed on ice and injected onto an ultraperformance liquid chromatography (UPLC) system immersed in ice. The protein was run over an immobilized pepsin column (Applied Biosystems, Poroszyme, 2-3131-00) at 130 μl/min and collected over a particle van-guard precolumn (Waters) for 3 min. The trap was then eluted in line with an Acquity 1.7-μm particle, 100 mm × 1 mm C18 UPLC column (Waters) with a 5 to 36% gradient of buffer A (0.1% formic acid) and buffer B (100% acetonitrile) over 20 min, and injected onto a LTQ Orbitrap XL (Thermo Scientific) to acquire mass spectra of peptides ranging from 350 to 1500 *m/z*.

Protein digestion and peptide identification

Mass analysis of the peptide centroids was performed as described previously, using the software HD-Examiner (Sierra Analytics) (*16*). Initial peptide identification was done by running tandem MS/MS experiments using a 5 to 35% B gradient over 60 min with an LTQ Orbitrap XL (Thermo Scientific). Peptides were identified by Mascot search in Thermo Proteome Discoverer software v. 1.2 (Thermo Scientific) based on fragmentation and peptide mass. The MS tolerance was set at 3 parts per million (ppm), with an MS/MS tolerance of 0.5 daltons. All peptides with a Mascot score >15 were analyzed by the HD-Examiner software. Any ambiguous peptides were excluded from the analysis. The full list of peptides was then manually validated by searching a nondeuterated protein sample MS scan to test for correct *m/z* state and to check for the presence of overlapping peptides. The HD-Examiner software was used to automate the initial analysis of deuterium incorporation, but every peptide listed in the manuscript was manually verified at every state and time to check for correct charge state, *m/z* range, presence of overlapping peptides, and proper retention time.

Mass analysis of peptide centroids

Selected peptides were manually examined for deuterium incorporation and accurate identification. Results are presented as relative extent of deuteration with no correction for back exchange because no fully deuterated protein sample could be obtained. However, a correction was applied to compensate for differences in the amount of deuterium in the exchange buffer (78 or 69% in experiments with lipids). The real extent of deuteration was ~25 to 35% higher than what is shown, based on tests performed with fully deuterated standard peptides. The average error was ≤0.2 dalton for corrected data of two replicates. The deuterium incorporation was also plotted versus the on-exchange time. The 3 s at 0°C time point was labeled as 0.3 s. Because we performed the experiments with lipids at lower protein concentration to increase the lipid-to-protein ratio, some peptides analyzed for the fusion construct could no longer be analyzed.

Akt activation

HEK 293T or HEK 293E cells were grown in Dulbecco's modified Eagle's medium (DMEM) containing 10% FBS and transfected with plasmids encoding human p85α, wild-type or mutant human myc-p110β, and myc-Akt with or without plasmids encoding FLAG-tagged $Gβ_1$ (FLAG-$Gβ_1$) and hemagglutinin-tagged $Gγ_2$ (HA-$Gγ_2$), as indicated. Cells were incubated overnight in serum-free medium. N-myristoylated peptides (wild type: KAAEIASSDSANVSSRGGKKFLPV; scrambled: NGAEKVGSADSKSIAFVSLKARSP; 50 mM stock in DMSO; final concentration, 30 μM), wortmannin (100 nM), PIK-75 (10 nM), and TGX-221 (50 nM) were added to the medium for 30 min before lysis of cells. After incubation, cells were lysed and subjected to immunoprecipitation with anti-myc antibodies. Lysates and immunoprecipitates were analyzed by Western blotting for Akt and pT^{308}-Akt with specific antibodies (Cell Signaling Technologies) and were analyzed by enhanced chemiluminesence (GE Healthcare) followed by densitometry or with the LI-COR Odyssey imaging system. Results are shown as the ratio of the abundance of pAkt to that of total Akt.

Transformation assays

NIH 3T3 cells grown in DMEM containing 10% normal calf serum were transfected with plasmids encoding p110β and p85α constructs. Two days after transfection, cells (2500 cells per well) were plated in 1 ml of 0.3% top agar over 1 ml of 0.6% bottom agar in a six-well dish. Cell colonies were counted 3 weeks later. In assays with the myristoylated peptides, peptides were diluted to a concentration of 30 μM in both the top and bottom gels as well as in the media.

Focus formation assays

NIH 3T3 cells were plated (at 2×10^5 cells per well) in six-well dishes and were transfected with plasmids encoding myc-p110β and p85α constructs. Cells were grown for 2 weeks, with medium changed every 2 days. The cells were fixed and stained with crystal violet, and the numbers of foci per well were counted. In assays with the myristoylated peptides, peptides were diluted to a concentration of 30 μM in the media for the duration of the assay.

Rab5 pulldown assays

HEK 293T cells were transfected with FuGENE HD with plasmids encoding wild-type or mutant myc-p110β and p85α. The cells were washed with cold PBS and lysed in 120 mM NaCl, 20 mM tris (pH 7.5), 1 mM $MgCl_2$, 1 mM $CaCl_2$, 10% glycerol, 1% NP40, containing EDTA-free protease inhibitor cocktail (Roche), and phosphatase inhibitor cocktails 1 (EMD) and 2 (Sigma). Lysates were incubated with GTPγS-Rab5 or GST beads as previously described (*43*) and washed, and bound proteins were eluted and analyzed by Western blotting.

Boyden chamber assays

NIH 3T3 cells, NIH 3T3 cells stably expressing wild-type or mutant p110β, or PC-3 cells were plated at 5×10^4 cells on tissue culture inserts containing 8.0-μm pores. The inserts were incubated with serum-free medium in the presence of DMSO or myristoylated peptides (30 μM) in the

upper chamber and medium containing DMSO or peptides with 10% FBS in the lower chamber. After 24 hours, the cells were fixed in 4% paraformaldehyde (PFA). The insert membranes were removed, stained, and mounted on coverslips with Dapi Fluoromount (Southern Biotech). Images were collected at 10× magnification with a Nikon Diaphot inverted fluorescence microscope and a SPOT Idea digital camera and were analyzed using ImageJ software.

MTT cell proliferation assays

The 3-(4,5-dimethylthiazol-2-yl)-2,5-diphenyltetrazolium bromide (MTT) assay (Invitrogen) was performed as described by the manufacturer. Briefly, 1×10^3 cells were plated in 96-well plates in the appropriate medium with or without DMSO or 30 μM myristoylated peptides. At various times, the cells were incubated with a 12 mM MTT solution in PBS for 4 hours at 37°C. An equal volume of SDS solution (0.1 g/ml) in 0.01 M HCl was added, and absorbance was read at 570 nm with a Spectramax M5 plate reader (Molecular Devices). The number of cells was calculated using the ratio of optical density/cell number determined from a known number of cells on day 1.

Collagen invasion assay

BAC-1.2F5 macrophages and PC-3 tumor cells were vitally labeled with CellTracker Red CMPTX and CellTracker Green CMFDA, respectively, and cocultured at a 2.5:1 ratio in a MatTek plate. After cell attachment, the cells were overlaid with a collagen I gel. Invasion into the three-dimensional gel was quantified after 24 hours by laser scanning confocal microscopy detection of the fluorescent signal from the red and green CellTracker dyes as described previously (*30*).

Adenylyl cyclase assay

Sf9 cells were infected with baculovirus coding for recombinant adenylyl cyclase 2. Sf9 cell membranes containing adenylyl cyclase 2 were prepared as previously described (*44*). Adenylyl cyclase activity was measured with the procedure described by Smigel (*45*). All assays were performed for 10 min at 30°C in a final volume of 100 μl containing 5 μg of cyclase-containing Sf9 membrane protein, 20 nM each of recombinant Gαs and Gβγ, and 30 μM of myristoylated p110β peptide or a previously described inhibitory QEHA peptide (QEHAQEPERQYMHIGTMVEFAYALVGK) (*46*). The data are means ± SD from duplicate determinations and are representative of two separate experiments.

LC3 puncta assays

HEK 293A cells stably expressing green fluorescent protein (GFP)–tagged LC3 were plated on poly-L-lysine–coated coverslips; treated with DMSO or myristoylated peptides (30 μM) for 30 min; and then incubated in PBS, 100 nM rapamycin, and peptide for 2 hours at 37°C. Coverslips were fixed in 4% PFA for 10 min at room temperature and then imaged with 60× 1.4 numerical aperture optics with a Nikon Eclipse E400 microscope. Images were collected with a Roper cooled charge-coupled device camera and analyzed with ImageJ software.

In vitro activation of PLC-β

L-α-Phosphatidylethanolamine (Avanti Polar Lipids, bovine liver), L-α-phosphatidylinositol-4,5-bisphosphate (Avanti, porcine brain), and [^{3}H]phosphatidylinositol-4,5-bisphosphate (NEN Radiochemicals) were combined in chloroform, dried under a stream of N_2, and resuspended in 20 mM Hepes (pH 7.2) by sonication. Recombinant PLC-β3 (1 nM) was incubated with the indicated concentrations of p110β peptide, scrambled peptide, or SIGK peptide, with or without 200 nM $G\alpha_q$ and in the presence or absence of 60 nM Gβγ, for 10 min at 30°C in a final volume of 60 μl containing 20 mM Hepes (pH 7.2), 8.3 mM NaCl, BSA (0.167 mg/ml), 2 mM DTT, 70 mM KCl, 3 mM EGTA, 10 mM NaF, 20 μM $AlCl_3$, 5 mM $MgCl_2$, 33 μM PIP_2, 333 μM PE, and 10,000 to 15,000 dpm of [^{3}H]PIP_2; $CaCl_2$ was added to give a free concentration of 200 nM Ca^{2+}. The assay was terminated by the addition of 200 μl of 10% trichloroacetic acid (TCA) and 100 μl of BSA (10 mg/ml), followed by centrifugation for 10 min at 4500*g*. The supernatant was quantified by liquid scintillation spectrometry.

Quantification of [^{3}H]inositol phosphate accumulation in cells

COS-7 cells were transiently transfected with or without plasmids encoding Gβγ subunits with FuGENE 6. The culture medium was changed about 48 hours after plating to inositol-free DMEM (MP Biomedical) containing [2-^{3}H(N)]myo-inositol (1 μCi per well) (American Radiolabeled Chemicals). Metabolic labeling proceeded for 18 hours, at which point 100 μl of myristoylated or TAT-labeled peptide (to a final concentration of 30 μM) was added. After 30 min, 50 mM LiCl in 20 mM Hepes (pH 7.2) was added for 1 hour at 37°C. Incubations were terminated by aspiration of media and the addition of ice-cold 50 mM formic acid, followed by neutralization with 150 mM NH_4OH after cell lysis. [^{3}H]Inositol phosphates were isolated and quantified by Dowex chromatography. Parallel dishes were lysed and assayed for Akt activation as described earlier.

Statistical analysis

Error bars show the SEM for experiments performed three or more times and the SD for experiments performed twice. Statistical analyses were performed by analysis of variance (ANOVA).

SUPPLEMENTARY MATERIALS

www.sciencesignaling.org/cgi/content/full/5/253/ra89/DC1

Fig. S1. Sequence alignment of p110α, p110β, and p110δ.
Fig. S2. Mapping of the Gβγ-binding region on p110β at the membrane with HDX-MS.
Fig. S3. Mapping of the Gβγ-binding region in p110β with HDX-MS.
Fig. S4. In vitro stimulation of PI3Kβ mutants by Gβγ.
Fig. S5. Activation of Akt in cells transfected with plasmids encoding PI3Kβ and Gβγ: inhibition by TGX221 and p110β-derived peptide.
Fig. S6. Pertussis toxin–sensitive effects of PI3Kβ.
Fig. S7. Peptides derived from p110β inhibit GPCR-mediated activation of p110β signaling in intact cells.
Fig. S8. Peptide inhibitors of Gβγ-mediated PI3Kβ activation are specific for p85-p110β.
Fig. S9. In vitro activity of heterodimers of p110β associated with p85 truncation constructs.
Table S1. Summary of all p110β peptides analyzed by HDX-MS for the p110β–p85α-icSH2 dimer (wild type) and for the p110β–Gβ-p85α-icSH2–Gγ-C68S (fusion) complexes.
Table S2. Summary of all p85 regulatory subunit peptides analyzed by HDX-MS for the p110β–p85α-icSH2 dimer (wild type) and for the p110β–Gβ-p85α-icSH2–Gγ-C68S (fusion) complexes.
Table S3. Summary of all peptide exchange data for the Gβ subunit for HDX-MS experiments with wild-type and fusion complexes.
Table S4. Summary of all peptide exchange data for the Gγ subunit for HDX-MS experiments with wild-type and fusion complexes.
Table S5. Summary of all p110β peptides analyzed by HDX-MS for PI3Kβ-pY with and without liposomes and Gβγ complexes.
Table S6. Summary of all p85 regulatory subunit peptides analyzed by HDX-MS for the PI3Kβ-pY with and without liposomes and Gβγ complexes.

REFERENCES AND NOTES

1. J. A. Engelman, Targeting PI3K signalling in cancer: Opportunities, challenges and limitations. *Nat. Rev. Cancer* **9**, 550–562 (2009).
2. J. Yu, Y. Zhang, J. McIlroy, T. Rordorf-Nikolic, G. A. Orr, J. M. Backer, Regulation of the p85/p110 phosphatidylinositol 3′-kinase: Stabilization and inhibition of the p110α catalytic subunit by the p85 regulatory subunit. *Mol. Cell. Biol.* **18**, 1379–1387 (1998).
3. B. Geering, P. R. Cutillas, G. Nock, S. I. Gharbi, B. Vanhaesebroeck, Class IA phosphoinositide 3-kinases are obligate p85-p110 heterodimers. *Proc. Natl. Acad. Sci. U.S.A.* **104**, 7809–7814 (2007).

4. S. Kulkarni, C. Sitaru, Z. Jakus, K. E. Anderson, G. Damoulakis, K. Davidson, M. Hirose, J. Juss, D. Oxley, T. A. Chessa, F. Ramadani, H. Guillou, A. Segonds-Pichon, A. Fritsch, G. E. Jarvis, K. Okkenhaug, R. Ludwig, D. Zillikens, A. Mocsai, B. Vanhaesebroeck, L. R. Stephens, P. T. Hawkins, PI3Kβ plays a critical role in neutrophil activation by immune complexes. *Sci. Signal.* **4**, ra23 (2011).
5. H. Kurosu, T. Maehama, T. Okada, T. Yamamoto, S. Hoshino, Y. Fukui, M. Ui, O. Hazeki, T. Katada, Heterodimeric phosphoinositide 3-kinase consisting of p85 and p110β is synergistically activated by the βγ subunits of G proteins and phosphotyrosyl peptide. *J. Biol. Chem.* **272**, 24252–24256 (1997).
6. C. Murga, S. Fukuhara, J. S. Gutkind, A novel role for phosphatidylinositol 3-kinase β in signaling from G protein-coupled receptors to Akt. *J. Biol. Chem.* **275**, 12069–12073 (2000).
7. U. Maier, A. Babich, B. Nürnberg, Roles of non-catalytic subunits in Gβγ-induced activation of class I phosphoinositide 3-kinase isoforms β and γ. *J. Biol. Chem.* **274**, 29311–29317 (1999).
8. S. Wee, D. Wiederschain, S. M. Maira, A. Loo, C. Miller, R. deBeaumont, F. Stegmeier, Y. M. Yao, C. Lengauer, PTEN-deficient cancers depend on PIK3CB. *Proc. Natl. Acad. Sci. U.S.A.* **105**, 13057–13062 (2008).
9. I. M. Berenjeno, J. Guillermet-Guibert, W. Pearce, A. Gray, S. Fleming, B. Vanhaesebroeck, Both p110α and p110β isoforms of PI3K can modulate the impact of loss-of-function of the PTEN tumour suppressor. *Biochem. J.* **442**, 151–159 (2012).
10. S. Jia, Z. Liu, S. Zhang, P. Liu, L. Zhang, S. H. Lee, J. Zhang, S. Signoretti, M. Loda, T. M. Roberts, J. J. Zhao, Essential roles of PI(3)K-p110β in cell growth, metabolism and tumorigenesis. *Nature* **454**, 776–779 (2008).
11. J. Ni, Q. Liu, S. Xie, C. Carlson, T. Von, K. Vogel, S. Riddle, C. Benes, M. Eck, T. Roberts, N. Gray, J. Zhao, Functional characterization of an isoform-selective inhibitor of PI3K-p110β as a potential anticancer agent. *Cancer Discov.* **2**, 425–433 (2012).
12. Z. Songyang, S. E. Shoelson, M. Chaudhuri, G. Gish, T. Pawson, W. G. Haser, F. King, T. Roberts, S. Ratnofsky, R. J. Lechleider, B. G. Neel, R. B. Birge, J. E. Fajardo, M. M. Chou, H. Hanafusa, B. Schaffhausen, L. C. Cantley, SH2 domains recognize specific phosphopeptide sequences. *Cell* **72**, 767–778 (1993).
13. R. O'Brien, P. Rugman, D. Renzoni, M. Layton, R. Handa, K. Hilyard, M. D. Waterfield, P. C. Driscoll, J. E. Ladbury, Alternative modes of binding of proteins with tandem SH2 domains. *Protein Sci.* **9**, 570–579 (2000).
14. H. A. Dbouk, H. Pang, A. Fiser, J. M. Backer, A biochemical mechanism for the oncogenic potential of the p110β catalytic subunit of phosphoinositide 3-kinase. *Proc. Natl. Acad. Sci. U.S.A.* **107**, 19897–19902 (2010).
15. X. Zhang, O. Vadas, O. Perisic, K. E. Anderson, J. Clark, P. T. Hawkins, L. R. Stephens, R. L. Williams, Structure of lipid kinase p110β/p85β elucidates an unusual SH2-domain-mediated inhibitory mechanism. *Mol. Cell* **41**, 567–578 (2011).
16. J. E. Burke, O. Vadas, A. Berndt, T. Finegan, O. Perisic, R. L. Williams, Dynamics of the phosphoinositide 3-kinase p110δ interaction with p85α and membranes reveals aspects of regulation distinct from p110α. *Structure* **19**, 1127–1137 (2011).
17. K. Y. Chung, S. G. Rasmussen, T. Liu, S. Li, B. T. DeVree, P. S. Chae, D. Calinski, B. K. Kobilka, V. L. Woods Jr., R. K. Sunahara, Conformational changes in the G protein Gs induced by the β_2 adrenergic receptor. *Nature* **477**, 611–615 (2011).
18. J. R. Engen, Analysis of protein conformation and dynamics by hydrogen/deuterium exchange MS. *Anal. Chem.* **81**, 7870–7875 (2009).
19. J. E. Burke, O. Perisic, G. R. Masson, O. Vadas, R. L. Williams, Oncogenic mutations mimic and enhance dynamic events in the natural activation of phosphoinositide 3-kinase p110α (PIK3CA). *Proc. Natl. Acad. Sci. U.S.A.* **109**, 15259–15264 (2012).
20. D. Mandelker, S. B. Gabelli, O. Schmidt-Kittler, J. Zhu, I. Cheong, C. H. Huang, K. W. Kinzler, B. Vogelstein, L. M. Amzel, A frequent kinase domain mutation that changes the interaction between PI3Kα and the membrane. *Proc. Natl. Acad. Sci. U.S.A.* **106**, 16996–17001 (2009).
21. M. Sun, J. R. Hart, P. Hillmann, M. Gymnopoulos, P. K. Vogt, Addition of N-terminal peptide sequences activates the oncogenic and signaling potentials of the catalytic subunit p110α of phosphoinositide-3-kinase. *Cell Cycle* **10**, 3731–3739 (2011).
22. U. Maier, A. Babich, N. Macrez, D. Leopoldt, P. Gierschik, D. Illenberger, B. Nurnberg, $G\beta_5\gamma_2$ is a highly selective activator of phospholipid-dependent enzymes. *J. Biol. Chem.* **275**, 13746–13754 (2000).
23. E. Buck, J. Li, Y. Chen, G. Weng, S. Scarlata, R. Iyengar, Resolution of a signal transfer region from a general binding domain in Gβ for stimulation of phospholipase C–β2. *Science* **283**, 1332–1335 (1999).
24. M. P. Panchenko, K. Saxena, Y. Li, S. Charnecki, P. M. Sternweis, T. F. Smith, A. G. Gilman, T. Kozasa, E. J. Neer, Sites important for PLCβ2 activation by the G protein βγ subunit map to the sides of the β propeller structure. *J. Biol. Chem.* **273**, 28298–28304 (1998).
25. J. K. Scott, S. F. Huang, B. P. Gangadhar, G. M. Samoriski, P. Clapp, R. A. Gross, R. Taussig, A. V. Smrcka, Evidence that a protein-protein interaction 'hot spot' on heterotrimeric G protein βγ subunits is used for recognition of a subclass of effectors. *EMBO J.* **20**, 767–776 (2001).
26. Y. Li, P. M. Sternweis, S. Charnecki, T. F. Smith, A. G. Gilman, E. J. Neer, T. Kozasa, Sites for Gα binding on the G protein β subunit overlap with sites for regulation of phospholipase Cβ and adenylyl cyclase. *J. Biol. Chem.* **273**, 16265–16272 (1998).
27. A. Shymanets, M. R. Ahmadian, K. T. Kossmeier, R. Wetzker, C. Harteneck, B. Nurnberg, The p101 subunit of PI3Kγ restores activation by Gβ mutants deficient in stimulating p110γ. *Biochem. J.* **441**, 851–858 (2012).
28. Z. Dou, M. Chattopadhyay, J. A. Pan, J. L. Guerriero, Y. P. Jiang, L. M. Ballou, Z. Yue, R. Z. Lin, W. X. Zong, The class IA phosphatidylinositol 3-kinase p110-β subunit is a positive regulator of autophagy. *J. Cell Biol.* **191**, 827–843 (2010).
29. A. L. Bookout, A. E. Finney, R. Guo, K. Peppel, W. J. Koch, Y. Daaka, Targeting Gβγ signaling to inhibit prostate tumor formation and growth. *J. Biol. Chem.* **278**, 37569–37573 (2003).
30. S. Goswami, E. Sahai, J. B. Wyckoff, M. Cammer, D. Cox, F. J. Pixley, E. R. Stanley, J. E. Segall, J. S. Condeelis, Macrophages promote the invasion of breast carcinoma cells via a colony-stimulating factor-1/epidermal growth factor paracrine loop. *Cancer Res.* **65**, 5278–5283 (2005).
31. R. Lappano, M. Maggiolini, G protein-coupled receptors: Novel targets for drug discovery in cancer. *Nat. Rev. Drug Discov.* **10**, 47–60 (2011).
32. R. T. Dorsam, J. S. Gutkind, G-protein-coupled receptors and cancer. *Nat. Rev. Cancer* **7**, 79–94 (2007).
33. Y. Daaka, G proteins in cancer: The prostate cancer paradigm. *Sci. STKE* **2004**, re2 (2004).
34. N. Macrez, C. Mironneau, V. Carricaburu, J. F. Quignard, A. Babich, C. Czupalla, B. Nürnberg, J. Mironneau, Phosphoinositide 3-kinase isoforms selectively couple receptors to vascular L-type Ca^{2+} channels. *Circ. Res.* **89**, 692–699 (2001).
35. S. P. Jackson, S. M. Schoenwaelder, I. Goncalves, W. S. Nesbitt, C. L. Yap, C. E. Wright, V. Kenche, K. E. Anderson, S. M. Dopheide, Y. Yuan, S. A. Sturgeon, H. Prabaharan, P. E. Thompson, G. D. Smith, P. R. Shepherd, N. Daniele, S. Kulkarni, B. Abbott, D. Saylik, C. Jones, L. Lu, S. Giuliano, S. C. Hughan, J. A. Angus, A. D. Robertson, H. H. Salem, PI 3-kinase p110β: A new target for antithrombotic therapy. *Nat. Med.* **11**, 507–514 (2005).
36. E. Ciraolo, F. Morello, R. M. Hobbs, F. Wolf, R. Marone, M. Iezzi, X. Lu, G. Mengozzi, F. Altruda, G. Sorba, K. Guan, P. P. Pandolfi, M. P. Wymann, E. Hirsch, Essential role of the p110β subunit of phosphoinositide 3-OH kinase in male fertility. *Mol. Biol. Cell* **21**, 704–711 (2010).
37. Y. Leverrier, K. Okkenhaug, C. Sawyer, A. Bilancio, B. Vanhaesebroeck, A. J. Ridley, Class I phosphoinositide 3-kinase p110β is required for apoptotic cell and Fcγ receptor-mediated phagocytosis by macrophages. *J. Biol. Chem.* **278**, 38437–38442 (2003).
38. S. P. Jackson, S. M. Schoenwaelder, PI 3-kinase p110β regulation of platelet integrin α(IIb)β3. *Curr. Top. Microbiol. Immunol.* **346**, 203–224 (2010).
39. E. Ciraolo, M. Iezzi, R. Marone, S. Marengo, C. Curcio, C. Costa, O. Azzolino, C. Gonella, C. Rubinetto, H. Wu, W. Dastrù, E. L. Martin, L. Silengo, F. Altruda, E. Turco, L. Lanzetti, P. Musiani, T. Rückle, C. Rommel, J. M. Backer, G. Forni, M. P. Wymann, E. Hirsch, Phosphoinositide 3-kinase p110β activity: Key role in metabolism and mammary gland cancer but not development. *Sci. Signal.* **1**, ra3 (2008).
40. A. Kumar, O. Fernandez-Capetillo, A. C. Carrera, Nuclear phosphoinositide 3-kinase β controls double-strand break DNA repair. *Proc. Natl. Acad. Sci. U.S.A.* **107**, 7491–7496 (2010).
41. D. Leopoldt, T. Hanck, T. Exner, U. Maier, R. Wetzker, B. Nürnberg, Gβγ stimulates phosphoinositide 3-kinase-γ by direct interaction with two domains of the catalytic p110 subunit. *J. Biol. Chem.* **273**, 7024–7029 (1998).
42. Z. A. Knight, M. E. Feldman, A. Balla, T. Balla, K. M. Shokat, A membrane capture assay for lipid kinase activity. *Nat. Protoc.* **2**, 2459–2466 (2007).
43. S. Christoforidis, M. Zerial, Purification and identification of novel Rab effectors using affinity chromatography. *Methods* **20**, 403–410 (2000).
44. R. Taussig, W. J. Tang, A. G. Gilman, Expression and purification of recombinant adenylyl cyclases in Sf9 cells. *Methods Enzymol.* **238**, 95–108 (1994).
45. M. D. Smigel, Purification of the catalyst of adenylate cyclase. *J. Biol. Chem.* **261**, 1976–1982 (1986).
46. J. Chen, M. DeVivo, J. Dingus, A. Harry, J. Li, J. Sui, D. J. Carty, J. L. Blank, J. H. Exton, R. H. Stoffel, J. Inglese, R. J. Lefkowitz, D. E. Logothetis, J. D. Hildebrandt, R. Iyengar, A region of adenylyl cyclase 2 critical for regulation by G protein βγ subunits. *Science* **268**, 1166–1169 (1995).

Acknowledgments: We thank C. S. Rubin, S. C. Almo, J. B. Bonnano, and P. Seneviratne for valuable discussions; M. Levy for the PC-3 cell line; S. Tooze for the GFP-LC3 stable cell line; W.-X. Zong for assistance with the Rab5 pulldown assays; and S. B. Horwitz for the panel of endometrial cancer cell lines. We also thank F. Begum and S.-Y. Peak-Chew for help with the HDX-MS setup, J. Morrow for assistance with HD-examiner software, and R. Riehle for technical assistance with the purification of proteins. **Funding:** O.V. was supported by a Swiss National Science Foundation fellowship (grant no. PA00P3_134202) and a European Commission fellowship (FP7-PEOPLE-2010-IEF, no. 275880). J.E.B. was supported by an EMBO long-term fellowship (ALTF268-2009) and the British Heart Foundation (PG11/109/29247). H.A.D. and B.D.K. were supported by grants from the Janey Fund. R.S.S. was supported by NIH grant 5T32 GM007491 and by a National Research Service Award, 1 F31 AG040932-01. T.K.H. was supported by NIH grant GM57391. This

work was funded by NIH grants GM55692 (to J.M.B.) and PO1 CA 100324 (to J.M.B. and A.R.B.), by the Medical Research Council (to R.L.W., file reference U105184308), and by Deutsche Forschungsgemeinschaft (to B.N.). **Author contributions:** H.A.D. identified the potential Gβγ interaction site by sequence analysis; produced mutants; analyzed mutant construct activity; performed cell culture analysis of p110β mutants; conducted peptide inhibition experiments for signaling, Boyden chamber, and proliferation assays; prepared figures; and contributed to writing the paper. O.V. identified the potential Gβγ interaction site by HDX-MS, produced and purified PI3K mutants for in vitro activity assays and HDX-MS, carried out in vitro kinase assays, analyzed mutant construct activity, carried out all of the HDX-MS experiments, prepared figures, and contributed to writing the paper. A.S. expressed and purified proteins, including all of the Gβγ that was used for the HDX-MS, and conducted assays on recombinant p85/p110β. J.E.B. contributed to HDX-MS experiments and data analysis and helped revise the manuscript. R.S.S. analyzed p110β binding to Rab5. B.D.K. conducted Boyden chamber experiments. M.O.B. performed cell-based PLC-β experiments. G.L.W. performed in vitro PLC-β experiments. C.S. performed binding experiments with peptides and Gβγ subunits. C. Hsueh performed collagen invasion assays. O.P. contributed to cloning, expression, purification, and activity assays of p110β constructs and helped revise the manuscript. C. Harteneck contributed to expression, purification, and activity assays of Gβγ and PI3-kinases. P.R.S. supervised the synthesis of the PI3K inhibitors. T.K.H. supervised the PLC-β experiments and provided purified Gβγ. A.V.S. supervised binding experiments with peptides and Gβγ subunits. R.T. conducted the adenylyl cyclase assays. A.R.B. contributed to the design and analysis of chemotaxis and invasion assays. B.N. provided purified Gβγ for kinase assays and HDX-MS experiments, contributed to the design and analysis of assays on peptide and Gβγ effects on p110β activity of various PI3Kβ constructs, and contributed to writing of the manuscript. R.L.W. contributed to the design and analysis of the HDX-MS experiments and the p110β mutagenesis experiments and contributed to writing of the manuscript. J.M.B. contributed to the design and analysis of the p110β mutagenesis and the p110β activity and signaling experiments and contributed to writing of the manuscript. **Competing interests:** H.A.D. and J.M.B. have a patent pending on the development of therapeutics targeting the p110β-Gβγ interface. P.R.S. is a founder scientist of Pathway Therapeutics.

Submitted 29 May 2012
Accepted 14 November 2012
Final Publication 4 December 2012
10.1126/scisignal.2003264
Citation: H. A. Dbouk, O. Vadas, A. Shymanets, J. E. Burke, R. S. Salamon, B. D. Khalil, M. O. Barrett, G. L. Waldo, C. Surve, C. Hsueh, O. Perisic, C. Harteneck, P. R. Shepherd, T. K. Harden, A. V. Smrcka, R. Taussig, A. R. Bresnick, B. Nürnberg, R. L. Williams, J. M. Backer, G protein–coupled receptor–mediated activation of p110β by Gβγ is required for cellular transformation and invasiveness. *Sci. Signal.* **5**, ra89 (2012).